Super-twisting Sliding Mode Control of Container Cranes With Triangle-trapezoid Rope Reeving System

Mingxu Piao, Muhammad Umer Hameed Shah, Guanghao Huang, and Keum-Shik Hong*

International Journal of Control, Automation, and Systems 22(1) (2024) 16-26

ISSN:1598-6446 (print version)
eISSN:2005-4092 (electronic version)

To link to this article:
http://dx.doi.org/10.1007/s12555-023-0298-6

Springer

International Journal of Control, Automation, and Systems 22(1) (2024) 16-26
http://dx.doi.org/10.1007/s12555-023-0298-6
ISSN:1598-6446 eISSN:2005-4092
http://www.springer.com/12555

Super-twisting Sliding Mode Control of Container Cranes With Triangle-trapezoid Rope Reeving System

Mingxu Piao, Muhammad Umer Hameed Shah, Guanghao Huang, and Keum-Shik Hong*

Abstract: In this paper, the dynamics of a new type of container crane, in which eight ropes connect the trolley and spreader in a triangle-trapezoid shape, is developed. The triangle-trapezoid cable configuration for connecting the spreader with the trolley is introduced to reflect the dynamic aspects of the multi-rope reeving system. A super-twisting sliding mode control for the developed model is designed for accurate trolley position control and vibration suppression of the load. Due to its robustness property against external disturbance, satisfactory control performance is achieved. Finally, experimental results to validate the developed model and simulation results to verify the control algorithm are also provided in this study.

Keywords: Anti-sway control, container crane, modeling, sliding mode control, vibration suppression.

1. INTRODUCTION

In the past decades, rapid growth in the volume of international trade has been observed. Consequently, the competition within the logistics industry for more efficient and cost-effective services has intensified. It is known that more than 90% of the world's trade is done by sea. The success of maritime transports lies in that, compared with the freights through air and land, more extensive and heavier goods can easily be transported to far-distant places cheaply through large container ships. Recently, a new type of container crane equipped with a trolley-spreader system connected by eight ropes in a triangle-trapezoid configuration was introduced. Notably, the newly introduced mechanism improves safety and stability during container transportation. It is thus widely used in many container cranes, such as rail-mounted quay cranes, rail-mounted gantry cranes, and rubber-tired gantry cranes. This paper aims to model the dynamics of the container crane having a triangle-trapezoid rope reeving mechanism and designs a super-twisting sliding mode control law for the developed model.

Fig. 1 shows a typical rail-mounted gantry-type container crane and the newly introduced trolley-spreader mechanism focused in this paper. Fig. 2(a) depicts the side view of the rope reeving system in Fig. 1, in which eight ropes connect the trolley and the spreader. If the eight ropes are observed from the front-, back-, left-, and right-hand sides, one upside-down triangle contained in a trapezoid is seen. Therefore, we will call the rope reeving system in Fig. 2(a) a triangle-trapezoid rope reeving (TTRR) system. On the other hand, Fig. 2(b) shows the traditional rope reeving system and its pendulum motion. The trolley and spreader in the traditional case are also connected with eight ropes, but their side view is a parallelogram (i.e., two ropes per corner). However, in the new

(a) (b)

Fig. 1. (a) The rail-mounted gantry crane (RMGC) in this research and (b) its trolley-spreader system (Source: LIEBHERR, USA).

Manuscript received May 10, 2023; revised September 20, 2023; accepted October 24, 2023. Recommended by Associate Editor Chang-Sei Kim under the direction of Senior Editor Kyoung Kwan Ahn. This work was supported by the National Research Foundation of Korea under the Ministry of Science and ICT, Korea (grant no. RS-2023-00207954).

Mingxu Piao and Keum-Shik Hong are with the School of Mechanical Engineering, Pusan National University, 2 Busandaehak-ro, Geumjeong-gu, Busan 46241, Korea (e-mails: {piaomx, kshong}@pusan.ac.kr). Muhammad Umer Hameed Shah is with the College of Engineering and Information Technology, Ajman University, 346 Ajman, UAE (e-mail: m.shah@ajman.ac.ae). Guanghao Huang and Keum-Shik Hong are with the Institute for Future, School of Automation, Qingdao University, Qingdao 266071, China (e-mails: huangguanghao921@163.com, ksh@qdu.edu.cn).
* Corresponding author.

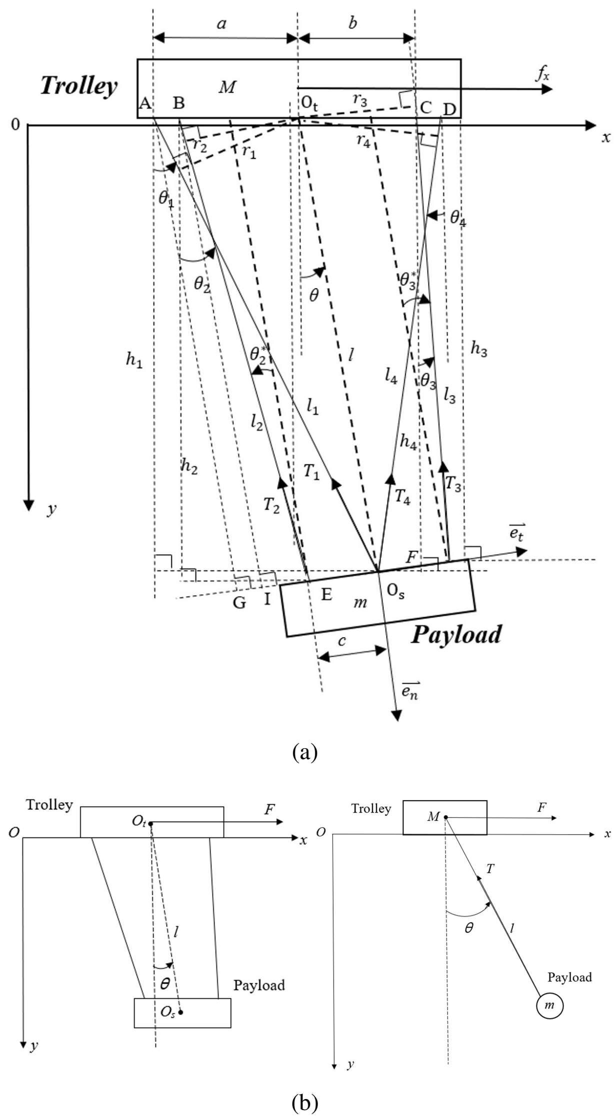

Fig. 2. Comparison of two rope reeving systems: (a) The triangle-trapezoid rope reeving system in Fig. 1 and (b) the conventional rope reeving system and its pendulum model.

configuration, a trapezoid shape made by the ropes is seen from each direction. This newly introduced TTRR system is more stable than the traditional reeving system. Because of the triangle shape's stability, the sway angle of the load during transportation and the residual sway angle at the end of transportation become smaller than the traditional mechanism. It is also seen from Fig. 2(a) that one side of the trolley has four support points (A, B, C, and D), and the corresponding side in the spreader has three support points (E, O_s, and F). Therefore, the spreader's orientation angles (trim, list, and skew) become much smaller than the traditional configuration in Fig. 2(b) due to the constraint forces that occurred along the ropes in the new mechanism. It is noted that the conventional mechanism has two support points on each side.

Since the TTRR system in Fig. 1 was introduced in the port industry about twenty years ago, no one has yet addressed the modeling of this new mechanism. The TTRR's effectiveness has been acknowledged by drivers' manual operations and remote operations from a control center. However, the same conclusion for an automated crane operation has not been drawn yet: A control algorithm for the new mechanism has not been fully developed yet.

In contrast, various control algorithms for the traditional rope reeving system (i.e., trapezoidal type) were reported. From a practical viewpoint, an automatic control algorithm based on an unreliable mathematical model cannot guarantee satisfactory control performance, which also results in unwanted oscillations of the container under slight disturbance.

In recent years, a considerable amount of research on the modeling and control of various cranes has been done. Hong and Shah [1] described a wide range of control models employed for most types of industrial cranes. Wijanand *et al.* [2] developed a coupled PDE-ODE system describing the motion of overhead cranes with a flexible cable. Xing and Liu [3] developed a 3D PDE overhead crane model with a variable-length flexible cable by preserving high-frequency modes. Golovin *et al.* [4] developed hybrid dynamics of a 2D overhead crane and a flexible leg for large gantry cranes. Xing *et al.* [5] modeled an overhead crane bridge subject to actuator failures and output constraints, in which the vertical vibration of the bridge was considered. Arena *et al.* [6] developed a 3D model (for dynamics analysis) of a container crane assuming four ropes connecting four corner points of the trolley and spreader. Lu *et al.* [7,8] modeled a 2D overhead crane system having dual trolleys, in which two ropes were used to connect each trolley and a position in the spreader. Another 2-rope model of container crane systems was developed by considering the trim motion of the spreader by Caporali [9]. Shi *et al.* [10] developed a double pendulum system for gantry cranes. Kim *et al.* [11] developed a dynamic model of the crane system transporting an underwater object and proposed a neural network-based robust anti-sway controller. A 3D model of tower cranes was developed by Liu *et al.* [12]. Ngo *et al.* [13] developed a dynamic model of container cranes for fuzzy sliding mode control. Hong and Ngo [14] developed a 3D mathematical model of a ship-mounted container crane (i.e., a mobile harbor) and validated it through experiments. However, all the works above have dealt with cranes having the rope reeving in Fig. 2(b).

Over the past years, many anti-sway control methods were developed for transporting cargo to target positions rapidly and without residual vibrations. Input shaping control is the most widely used open-loop control method among crane control techniques [15-22]. However, since the open loop control method does not have the ability to overcome the modeling uncertainty and disturbance problem, diverse feedback control methods have been developed for various applications, including adaptive control [23-29], fuzzy control [29-35], sliding mode control (SMC) [31,32,36-41], super-twisting control [42-44] and many other control methods [45-55]. Recently, SMC appeared as an effective control method in the cargo handling industry, which is a nonlinear control technique characterized by robustness against uncertainty and disturbance. SMC is designed to force the system's state to a specific surface in the state space called the sliding surface. Once the sliding surface is reached, the system's state is maintained in the vicinity of the sliding surface, and the dynamic characteristics of the closed-loop control are robust against the uncertainty, disturbance, and nonlinearity of the model. Because of these advantages, SMC is one of the promising control methods to overcome disturbances like winds. Hong and Ngo [36] have developed a sliding mode controller for a ship-mounted container crane. Adaptive sliding mode control methods have been applied to an overhead container crane system [23,24]. Nguyen *et al*. [27] developed an adaptive robust control scheme for electro-hydraulic servo systems. Yang *et al*. [28] developed an adaptive controller to address output and velocity constraints for actuated and unactuated variables together. An adaptive fuzzy control for a class of MIMO underactuated tower crane and double-pendulum systems is developed by Yang *et al*. [29]. Fuzzy sliding mode control has been utilized to control a container crane by Ngo *et al*. [31] for a mobile harbor crane system [32]. Wang and Chen [37] developed an observer-based sliding mode controller for mismatched uncertain systems. An adaptive terminal sliding mode controller for path-following control of nonlinear systems is developed by Truong *et al*. [38]. An extended sliding mode observer-based backstepping control strategy is developed by Nguyen *et al*. [39] for uncertain electro-hydraulic systems. Tran *et al*. [40] applied the adaptive sliding mode technique in the backstepping controller for the position tracking of an electrohydraulic elastic manipulator. Xu *et al*. [41] developed a backstepping sliding mode controller based on an extended state observer for robotic manipulators.

Although the SMC technique is very effective for swing suppression, the crane control system easily suffers from the chattering phenomena in the control input. This chattering phenomenon causes inaccuracy of control and is undesirable regarding the system's stability. For this issue, super-twisting control technology was proposed to reduce the chattering problem while guaranteeing the robustness property. Vazquez *et al*. [42] developed a super-twisting controller for the parametrically excited overhead crane system for the crane application. Sun *et al*. [43] presented a super-twisting-based nonlinear control law to make the crane follow preset trajectories and eliminate the swing angle of the double pendulum crane system. Moreno *et al*. [44] provided a method to construct a family of strict Lyapunov functions with a negative derivative for the super-twisting algorithm. A model predictive control method is developed and applied to the tower cranes and boom cranes by Zhai *et al*. [45]. Most existing works are still based on the trapezoidal type rope reeving system in Fig. 2(b) and its simple pendulum model on the right-hand side. Therefore, the underlining mechanics of the TTRR configuration and a more sophisticated control logic based on the developed model need to be developed.

The contributions of this study are the following. i) Considering the rope tension, a new mathematical model of container cranes with the TTRR configuration is developed for the first time. Then, the developed model is validated by comparing experimental data of a rail-mounted gantry crane and simulation data. ii) A super-twisting sliding mode control algorithm, based on the developed TTRR model, is designed to control the trolley position and suppress the payload vibration. A comprehensive simulation study is also performed to verify the effectiveness of the proposed control algorithm.

This paper is organized as follows: Section 2 discusses the mathematical modeling of the container crane with a triangle-trapezoid shape. In Section 3, a super-twisting sliding mode anti-sway control method is presented. Experimental and simulation results are given in Section 4. Finally, conclusions are made in Section 5.

2. MODELING

In this section, the trolley-spreader system with a triangle-trapezoid rope reeving mechanism in Fig. 2(a) is mathematically modeled: M and m are the masses of the trolley and the payload (including a spreader and the container), respectively; x is the trolley position in the positive direction; O_t and O_s are the center points of the trolley and spreader (the subscripts t and s stand for trolley and spreader), respectively; l is the distance between O_t and O_s; l_1, l_2, l_3, and l_4 are the rope lengths connecting four positions (A, B, C, and D) in the trolley and three positions (E, F, and O_s) in the spreader; a is the length of AO_t, which is the same as DO_t; b is the length of BO_t, which is the same as CO_t; c is the distance between E and O_s; θ, θ_1, θ_2, θ_3, and θ_4 are the angles between l, l_1, l_2, l_3, l_4 and the vertical direction; θ_2^* is the angle between l and l_2; θ_3^* is the angle between l and l_3; T_1, T_2, T_3, and T_4 are the tension forces of the corresponding ropes; $\bar{e}_t$ and $\bar{e}_n$ are the unit vectors of the tangential and normal forces about l; and let f_x be the control force in the x direction.

The equations of motion of the crane with the triangle-trapezoid rope reeving mechanism are derived as follows:

$$(M+m)\ddot{x}+ml\ddot{\theta}-ml\dot{\theta}^2\sin\theta = f_x+q_x, \tag{1}$$

$$ml^2\ddot{\theta}+ml\ddot{x}+mgl\sin\theta = q_\theta, \tag{2}$$

where

$$q_x = -T_1 \sin\theta_1 - T_2 \sin\theta_2 + T_3 \sin\theta_3 + T_4 \sin\theta_4, \quad (3)$$

$$q_\theta = -T_1 r_1 - T_2 r_2 + T_3 r_3 + T_4 r_4, \quad (4)$$

and

$$\sin\theta_1 = (a + l\sin\theta)/l_1, \quad (5)$$

$$\sin\theta_2 = (b + l\sin\theta - c\cos\theta)/l_2, \quad (6)$$

$$\sin\theta_3 = (l\sin\theta + c\cos\theta - b)/l_3, \quad (7)$$

$$\sin\theta_4 = (l\sin\theta - a)/l_4, \quad (8)$$

$$l_1 = ((AG)^2 + (GO_s)^2)^{1/2} = (l^2 + 2al\sin\theta + a^2)^{1/2}, \quad (9)$$

$$l_1 = ((AG)^2 + (GO_s)^2)^{1/2} = (l^2 + 2al\sin\theta + a^2)^{1/2}. \quad (10)$$

The following kinematic equations are obtained from Fig. 2(a).

$$l_3 = (l^2 + b^2 + c^2 - 2bl\sin\theta - 2bc\cos\theta)^{1/2}, \quad (11)$$

$$l_4 = (l^2 - 2al\sin\theta + a^2)^{1/2}. \quad (12)$$

Let h_i ($i = 1, 2, 3, 4$) be the vertical heights of the ith rope to the horizontal plane of the trolley, which are obtained as follows:

$$h_1 = h_4 = l\cos\theta, \quad (13)$$

$$h_2 = h_1 + c\sin\theta = l\cos\theta + c\sin\theta, \quad (14)$$

$$h_3 = h_2 - c\sin\theta = l\cos\theta - c\sin\theta. \quad (15)$$

Let r_i be the perpendicular distance between the center of the trolley O_t and the ith rope, which are obtained as follows:

$$r_1 = ah_1/l_1 = al\cos\theta/l_1, \quad (16)$$

$$r_2 = ah_2/l_2 = b(l\cos\theta + c\sin\theta)/l_2, \quad (17)$$

$$r_3 = ah_3/l_3 = b(l\cos\theta - c\sin\theta)/l_3, \quad (18)$$

$$r_4 = ah_4/l_4 = al\cos\theta/l_4. \quad (19)$$

If the payload is at the equilibrium position, the following relations hold.

$$l_{1e} = l_{4e},\ l_{2e} = l_{3e},\ T_{1e} = T_{4e},\ T_{2e} = T_{3e}, \quad (20)$$

$$T_{1e}\cos\theta_{1e} = T_{2e}\cos\theta_{2e} = T_{3e}\cos\theta_{3e} = T_{4e}\cos\theta_{4e} = mg/4, \quad (21)$$

where l_{ie} and T_{ie} are the rope length and tension of the ith rope at the equilibrium position, respectively, and θ_{ie} is the angle from the vertical direction to the ith rope at the equivalent position. Hooke's law is considered as follows:

$$\Delta T_i = AE\varepsilon_i = \frac{AE}{l_{i0}}\Delta l_i,\ i = 1,\ 2,\ 3,\ 4, \quad (22)$$

where A is the cross-sectional area, E is the modulus of elasticity, ε_i is the strain of the ith rope, Δl_i is the length change of the ith rope, ΔT_i is the tension force change of the ith rope, l_{i0} is the original length of the ith rope when it is not extended. The following relations are obtained.

$$\Delta l_i = l_i - l_{i0}, \quad (23)$$

$$T_{1e} = AE(l_{1e} - l_{10})/l_{10} = mg/4\cos\theta_{1e} = mgl_{1e}/4l, \quad (24)$$

$$l_{10} = 4AEll_{1e}/(mgl_{1e} + 4AEl) = l_{40}, \quad (25)$$

$$l_{20} = 4AEll_{2e}/(mgl_{2e} + 4AEl) = l_{30}, \quad (26)$$

where T_{ie} is the tension force of the ith rope at the equilibrium position. Then, the tension forces of individual ropes are obtained as follows:

$$T_i = T_{i0} + \Delta T_i, \quad (27)$$

$$T_1(\theta) = AE(l_1 - l_{10})/l_{1e}, \quad (28)$$

$$T_2(\theta) = T_{20} + \Delta T_2 = T_{20} + AE(-l_{20} + \sqrt{l^2 + b^2 + c^2 + 2bl\sin\theta - 2bc\cos\theta})/l_{20}, \quad (29)$$

$$T_3(\theta) = T_{30} + \Delta T_3 = T_{20} + AE(-l_{20} + \sqrt{l^2 + b^2 + c^2 - 2bl\sin\theta - 2bc\cos\theta})/l_{20}, \quad (30)$$

$$T_4(\theta) = T_{40} + \Delta T_4 = T_{40} + AE(-l_{40} + \sqrt{l^2 - 2al\sin\theta + a^2})/l_{40}. \quad (31)$$

Finally, q_x and q_θ in (3) and (4) are represented as follows:

$$q_x = -T_1(a + l\sin\theta)/l_1 - T_2(b + l\sin\theta - c)/l_2 + T_3(c + l\sin\theta - b)/l_3 + T_4(a - l\sin\theta)/l_4, \quad (32)$$

$$q_\theta = -T_1 al\cos\theta/l_1 - T_2 b(l\cos\theta + c\sin\theta)/l_2 + T_3 b(l\cos\theta - c\sin\theta)/l_3 + T_4 al\cos\theta/l_4. \quad (33)$$

Equations (32) and (33) are the main differences between the triangle-trapezoid rope reeving mechanism and the conventional single rope crane system. It is noted that these nonlinear terms make the swing motions more complex.

3. CONTROL DESIGN

In this section, a super-twisting sliding mode controller (STSMC) is developed to minimize the sway angle of the payload at the end of a trolley movement, improving safety and efficiency. This technique combines the advantages of sliding mode control and super-twisting control methods. Therefore, the developed control method is robust and achieves more smooth movement.

In this paper, the error vector for the controller is designed as follows:

$$e = [e_x \; e_\theta]^T = [x - x_d \;\; \theta - \theta_d]^T, \tag{34}$$

where e_x is the trolley position error, e_θ is the sway angular displacement error, x_d is the desired position of the trolley, θ_d is the desired payload sway angle. Since θ_d is designed to be zero, the sliding surface s is defined as follows:

$$s = k_0 \dot{e}_x + k_1 e_x - k_2 \theta, \tag{35}$$

where k_0, k_1, and k_2 are positive control gains. By differentiating (35), the following equation is obtained.

$$\dot{s} = k_0 \ddot{e}_x + k_1 \dot{e}_x - k_2 \dot{\theta}. \tag{36}$$

Now, from (2), $ml\ddot{\theta} = -m\ddot{x} - mg\sin\theta + q_\theta/l$, which is substituted for the second term in (1). Then, (1) becomes

$$\ddot{x} = (f_x + q_x + mg\sin\theta + ml\dot{\theta}^2\sin\theta - q_\theta/l)/M. \tag{37}$$

Assume that the sway angle is small, i.e., $\sin\theta \simeq \theta$. Let $\ddot{x}_d = \dot{x}_d = 0$. Then, (36) can be rewritten as follows:

$$\begin{aligned}\dot{s} &= k_0(f_x + q_x + mg\theta + ml\dot{\theta}^2\theta - q_\theta/l)/M + k_1\dot{x} \\ &\quad - k_2\dot{\theta} \\ &= F\left(x, \dot{x}, \theta, \dot{\theta}\right) + u,\end{aligned} \tag{38}$$

where F and u are defined as follows:

$$\begin{aligned}F &= k_0\left(q_x + mg\theta + ml\dot{\theta}^2\theta - q_\theta/l\right)/M + k_1\dot{x} \\ &\quad - k_2\dot{\theta},\end{aligned} \tag{39}$$

$$u = \frac{k_0}{M} f_x. \tag{40}$$

Since the crane system without control is a passive system, x, $\dot{x}$, θ and $\dot{\theta}$ are bounded. We further assume that F is bounded for some positive constant δ as follows:

$$\left|F\left(x, \dot{x}, \theta, \dot{\theta}\right)\right| \le \delta|s|^{1/2}, \; \delta > 0. \tag{41}$$

Now, the super-twisting sliding mode control law for (38) is designed as follows:

$$u = -k_3|s|^{1/2}\mathrm{sgn}(s) + u_1, \tag{42}$$

$$\dot{u}_1 = -k_4\mathrm{sgn}(s), \tag{43}$$

where k_3 and k_4 are positive control gains, u_1 is a designed intermediate variable. Equation (38) can be reformed by considering (42) and (43) as follows:

$$\dot{s} = F(x, \dot{x}, \theta, \dot{\theta}) - k_3|s|^{1/2}\mathrm{sgn}(s) + u_1. \tag{44}$$

A Lyapunov function candidate is designed as follows:

$$\begin{aligned}V &= 2k_4|s| + \frac{1}{2}u_1^2 + \frac{1}{2}(k_3|s|^{1/2}\mathrm{sgn}(s) - u_1)^2 \\ &= \frac{1}{2}(4k_4 + k_3^2)(|s|^{1/2}\mathrm{sgn}(s))^2 - \frac{1}{2}2k_3|s|^{1/2}\mathrm{sgn}(s)u_1 \\ &\quad + \frac{1}{2}2u_1^2 \\ &= \frac{1}{2}\begin{bmatrix}|s|^{1/2}\mathrm{sgn}(s) & u_1\end{bmatrix}\begin{bmatrix}4k_4 + k_3^2 & -k_3 \\ -k_3 & 2\end{bmatrix}\begin{bmatrix}|s|^{1/2}\mathrm{sgn}(s) \\ u_1\end{bmatrix} \\ &= \xi^T P \xi,\end{aligned} \tag{45}$$

where

$$P = \frac{1}{2}\begin{bmatrix}4k_4 + {k_3}^2 & -k_3 \\ -k_3 & 2\end{bmatrix}, \tag{46}$$

$$\xi^T = \begin{bmatrix}|s|^{1/2}\mathrm{sgn}(s) & u_1\end{bmatrix}. \tag{47}$$

Here, since u_1 can be obtained as $u + k_3|s|^{1/2}\mathrm{sgn}(s)$ from (42), (45) can be rewritten as $V = 2k_4|s| + u_1^2/2 + u^2/2$, which is continuous and differentiable. Now, we differentiate V in time (i.e., differentiate the terms after the second equality in (45)). Then, the following equation is obtained.

$$\dot{V} = -\xi^T Q \xi |s|^{-1/2} + F q^T \xi |s|^{-1/2}, \tag{48}$$

where

$$Q = \frac{k_3}{2}\begin{bmatrix}2k_4 + {k_3}^2 & -k_3 \\ -k_3 & 1\end{bmatrix}, \tag{49}$$

$$q^T = \begin{bmatrix}2k_4 + \frac{1}{2}{k_3}^2 & -\frac{1}{2}k_3\end{bmatrix}. \tag{50}$$

The following inequalities hold

$$|F| \le \delta|s|^{1/2} \le \delta\left\|\begin{bmatrix}|s|^{1/2}\mathrm{sgn}(s) & u_1\end{bmatrix}\right\|, \tag{51}$$

$$\begin{aligned}\left\|q^T\right\| &= \left\|\begin{bmatrix}2k_4 + \frac{1}{2}k_3^2 & -\frac{1}{2}k_3\end{bmatrix}\right\| \\ &< \frac{k_3}{2}\left\|\begin{bmatrix}\frac{4k_4}{k_3} + k_3 & -2 \\ -2 & 0\end{bmatrix}\right\|.\end{aligned} \tag{52}$$

Therefore, the second term $Fq^T\xi|s|^{-1/2}$ in (48) can be expressed as follows:

$$\begin{aligned}&F q^T \xi |s|^{-1/2} \\ &\le \frac{\delta k_3}{2}\begin{bmatrix}|s|^{1/2}\mathrm{sgn}(s) & u_1\end{bmatrix}\begin{bmatrix}\frac{4k_4}{k_3} + k_3 & -2 \\ -2 & 0\end{bmatrix}\begin{bmatrix}|s|^{1/2}\mathrm{sgn}(s) \\ u_1\end{bmatrix}.\end{aligned} \tag{53}$$

Substitute (53) into (48), then the following equation is obtained

$$\begin{aligned}\dot{V} &\le -|s|^{-1/2}\frac{k_3}{2}\begin{bmatrix}|s|^{1/2}\mathrm{sgn}(s) & u_1\end{bmatrix} \\ &\quad \times \begin{bmatrix}2k_4 + k_3^2 - (\frac{4k_4}{k_3} + k_3)\delta & -k_3 + 2\delta \\ -k_3 + 2\delta & 1\end{bmatrix}\begin{bmatrix}|s|^{1/2}\mathrm{sgn}(s) \\ u_1\end{bmatrix} \\ &= -|s|^{-1/2}\xi^T \bar{Q} \xi,\end{aligned} \tag{54}$$

where

$$\overline{Q} = \frac{k_3}{2}\begin{bmatrix}2k_4 + {k_3}^2 - (4k_4/k_3 + k_3)\,\delta & -k_3 + 2\delta \\ -k_3 + 2\delta & 1\end{bmatrix}. \tag{55}$$

Let the following conditions be satisfied

$$k_3 > 2\delta,\ k_4 > k_3(4\delta^2 - 3\delta k_3)/(2k_3 - 4\delta). \tag{56}$$

Then $|\overline{Q}| > 0$. Finally (54) can be represented as follows:

$$\dot{V} \leq -|s|^{-1/2}\xi^T\overline{Q}\xi \leq 0. \tag{57}$$

This implies that the derivative of the Lyapunov function candidate is negative semi-definite, assuring the uniform stability of the closed-loop system.

4. VALIDATION AND SIMULATION

4.1. Model validation

Fig. 3(a) depicts actual data obtained from a rail-mounted gantry crane (RMGC), showing the trolley position (the yellow thin line), the trolley velocity (the blue solid line), the sway angle (the yellow solid line), the sway angular velocity (the orange line). The payload height is known in this system, but the rope length information is unavailable. The time appears at the bottom of Fig. 3(a) (from 0 to 5,200), where each tick represents 0.01 seconds. In this experiment, $M = 40,000$ kg, $m = 2,000$ kg.

The swing period from this data is estimated to be 3.8 s. Therefore, the rope length is 3.588 m, using the period of a single pendulum, $T = 2\pi(l/g)^{1/2}$, where l is the rope length, and g is gravity acceleration. We now set $l = 3.588$ m in (1) and(2). The same trolley velocity (the blue line in Fig. 3(a)) is now applied to both the single pendulum and the triangle-trapezoid models. Fig. 3(b) compares the sway angles of the triangle-trapezoid model (the red solid line) and the pendulum model (the black dashed line). The yellow solid line in Fig. 3(a) is almost the same as the red solid line in Fig. 3(b), which reveals that the proposed model can reflect the RMGC's dynamics better than the single pendulum model. This is because the new model was developed by considering the position differences of individual pin joints and the reactive forces within the multi-rope system, which more accurately characterizes the new rope reeving system's dynamics.

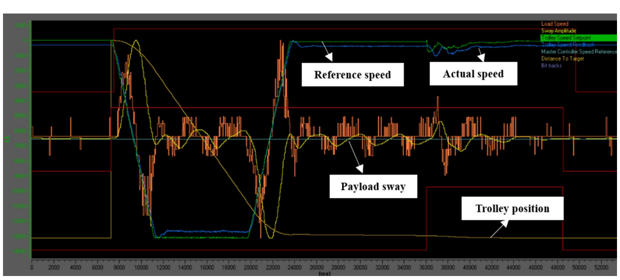

(a)

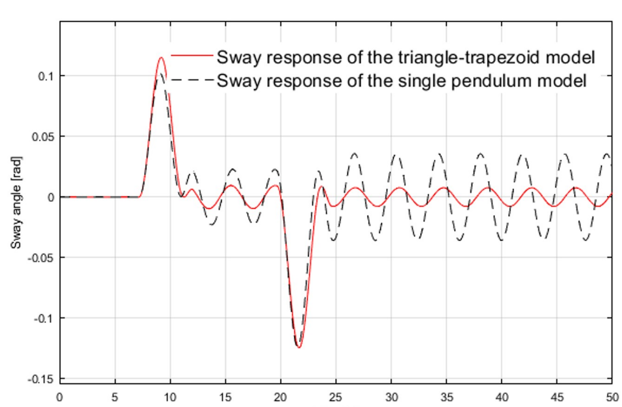

(b)

Fig. 3. Validation of the triangle-trapezoid model: (a) Experiment data and (b) simulation results.

4.2. STSMC simulation

In this section, the positive constant δ in (41) is set to 10 (by experience and was checked through simulation in advance). In this section, the control parameters are set as $k_0 = 800$, $k_1 = 500$, $k_2 = 11,000$, $k_3 = 200$, and $k_4 = 20$, which satisfy the relationship in (50). The angular acceleration disturbance was applied to the payload at 28 s, shown in Fig. 4. The payload mass varied from 2,000 kg (without a container) in Figs. 5 and 6, and 10,000 kg (with a container) in Figs. 7 and 8. The rope length is selected as 3.588 m, which corresponds to the payload's height at 20 m.

The trolley distance and the sway angle responses of the input shaping control [19] for the pendulum model and the triangle-trapezoid model are shown together with the sway angle response of the STSMC for the triangle-trapezoid model in Figs. 5 and 7. Figs. 6 and 8 show the trolley distances and the payload sway angle responses considering the angular acceleration disturbance shown in Fig. 4.

The simulation results in this section demonstrate that the newly developed mathematical model is proper for the triangle-trapezoidal rope reeving system. From Figs. 5-8, we can conclude that the proposed STSMC based on the

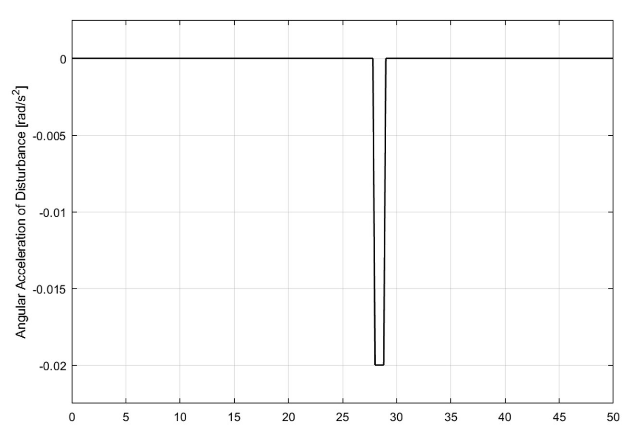

Fig. 4. Angular acceleration disturbance to the payload.

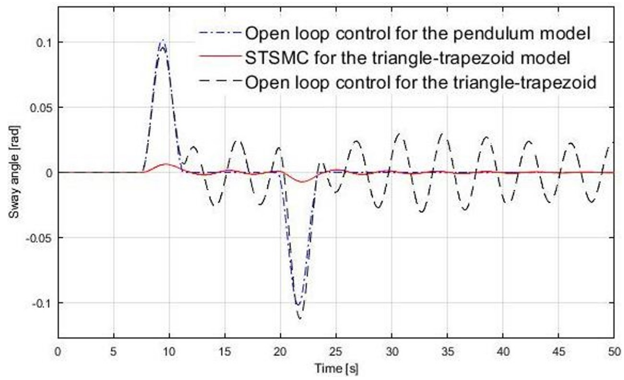

(a)

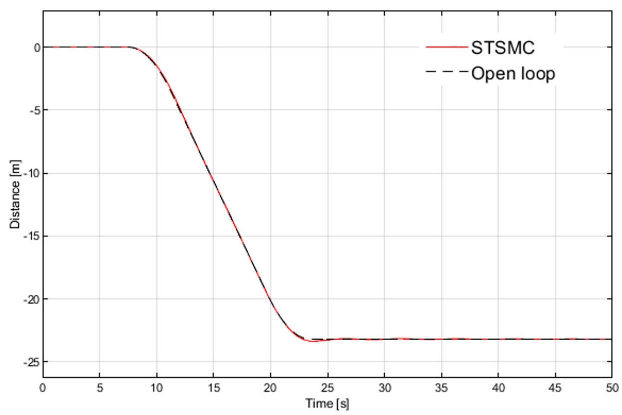

(b)

Fig. 5. Without disturbance ($L = 3.588$ m, $m = 2,000$ kg): (a) Sway angles of the payload and (b) traveling distances of the trolley.

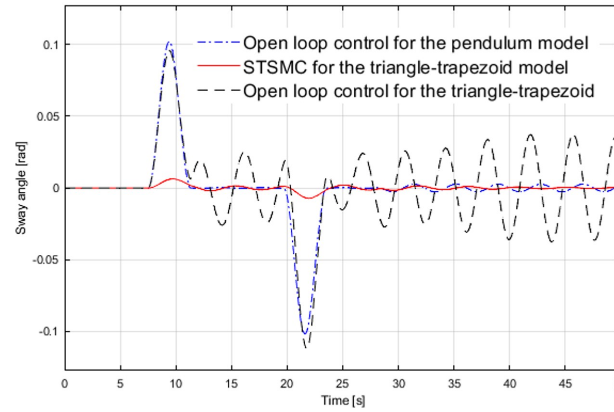

(a)

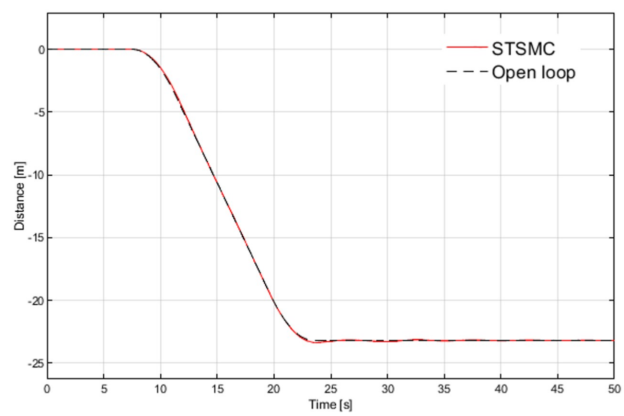

(b)

Fig. 6. With disturbance ($L = 3.588$ m, $m = 2,000$ kg): (a) Sway angles and (b) traveling distances.

new model has a better residual sway control effect and is more robust than the input shaping controller based on the single rope model without losing the trolley's traveling time. This is because the STSMC is developed based on the new mathematical model in Section 3, while the input shaping control method is designed based on the natural frequency of the single pendulum model, which is unsuitable for the triangle-trapezoid system.

By comparing Figs. 5(a) and 6(a) as well as Figs. 7(a) and 8(a), it is evident that, for the open-loop control, the residual vibration responses are much different with and without disturbance. However, the effects of disturbances will be forced to 0 quickly by utilizing STSMC, which means the developed control method can solve the angular disturbance problem effectively.

Fig. 9 compares the sway angle and the trolley distance of the STSMC and a PD control with the following control law.

$$f_{PD} = k_5(y_d - y) - k_6(\dot{y} - \dot{y}_d) + k_7\theta + k_8\dot{\theta}, \qquad (58)$$

where f_{PD} is the control input to the trolley in the x direction, and k_5, k_6, k_7, and k_8 are positive constants. It can be seen from Fig. 9 that the sway angle of the payload with the STSMC is much smaller than the one with the PD control. Overall, the STSMC is more effective for the researched TTRR system.

5. CONCLUSION

In this paper, a mathematical model of the triangle-trapezoidal rope reeving system was developed to control the modern crane systems effectively. The correctness of the model was verified by comparing the practical crane operation data with the simulation results based on the proposed model. For effective anti-sway control, a super-twisting sliding mode control method was developed. The simulation results validated the effectiveness of the developed control algorithm. The future work will focus on developing the 3D mathematical model based on the spreader rope reeving system and its control design.

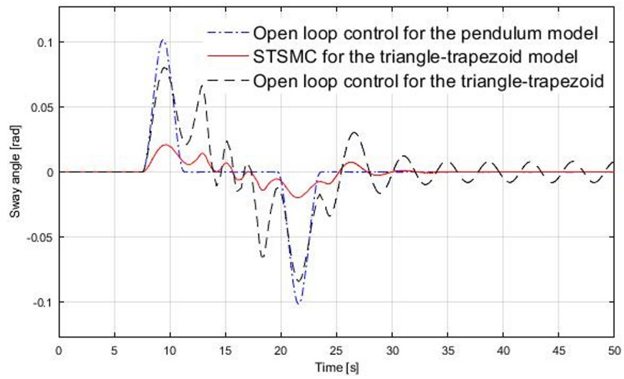

(a)

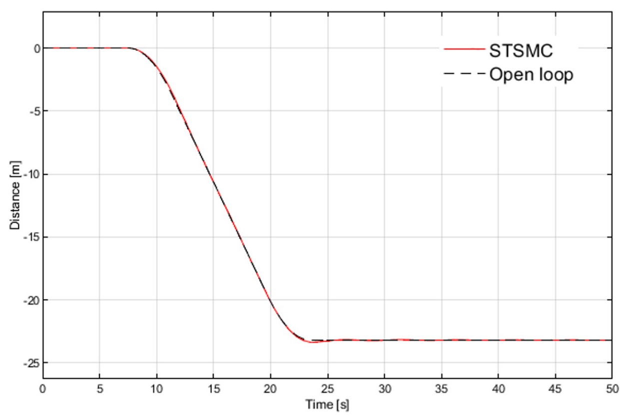

(b)

Fig. 7. Without disturbance ($L = 3.588$ m, $m = 10,000$ kg): (a) Sway angles and (b) traveling distances.

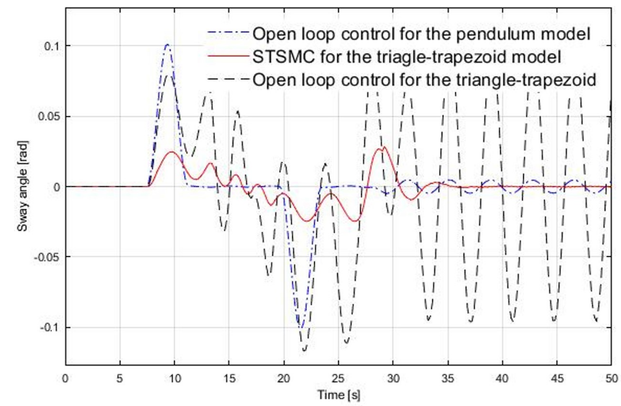

(a)

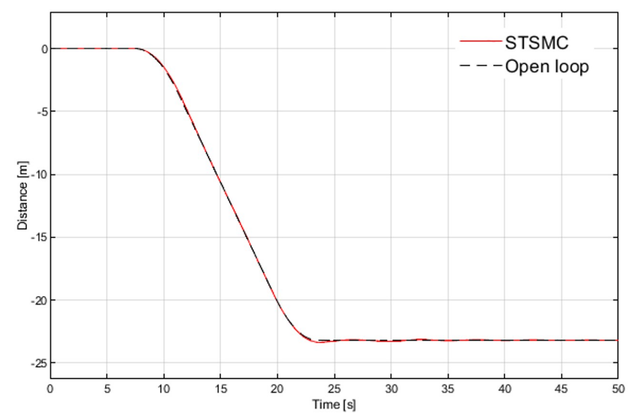

(b)

Fig. 8. With disturbance ($L = 3.588$ m, $m = 10,000$ kg): (a) Sway angles and (b) traveling distances.

CONFLICT OF INTEREST

The authors declare that they have no conflict of interest.

REFERENCES

[1] K.-S. Hong and U. H. Shah, *Dynamics and Control of Industrial Cranes*, Springer, ISBN 9789811357695, 2019.

[2] M. Wijnand, B. d'Andréa-Novel, and L. Rosier, "Finite-time stabilization of an overhead crane with a flexible cable submitted to an affine tension," *ESAIM: Control, Optimisation and Calculus of Variations*, vol. 27, no. 94, 2021.

[3] X. Xing and J. Liu, "Vibration and position control of overhead crane with three-dimensional variable length cable subject to input amplitude and rate constraints," *IEEE Transactions on System, Man, and Cybernetics: Systems*, vol. 51, no. 7, pp. 4127-4138, 2021.

[4] I. Golovin, A. Maksakov, M. Shysh, and S. Palis, "Discrepancy-based control for positioning of large gantry crane," *Mechanical Systems and Signal Processing*, vol. 163, no. 15, 2022.

[5] X. Y. Xing, H. J. Yang, and J. Liu, "Vibration control for nonlinear overhead crane bridge subject to actuator failures and output constraints," *Nonlinear Dynamics*, vol. 101, pp. 419-438, 2020.

[6] A. Arena, A. Casalotti, W. Lacarbonara, and M. P. Cartmell, "Dynamics of container cranes: Three-dimensional modeling, full-scale experiments, and identification," *International Journal of Mechanical Sciences*, vol. 93, pp. 8-21, 2015.

[7] B. Lu, Y. C. Fang, and N. Sun, "Modeling and nonlinear coordination control for an underactuated dual overhead crane system," *Automatica*, vol. 91, pp. 244-255, 2018.

[8] B. Lu, Y. C. Fang, and N. Sun, "Nonlinear control for underactuated multi-rope cranes: modeling, theoretical design and hardware experiments," *Control Engineering Practice Automation and Systems*, vol. 76, pp. 123-132, 2018.

[9] R. P. L. Caporali, "Overhead crane: an adaptive particle filter for anti-sway closed-loop and collision detection using computer vision," *International Journal of Innovative Computing, Information and Control*, vol. 15, no. 4, pp. 1223-1241, 2019.

[10] H. Shi, F. Yao, Z. Yuan, Y. Hu, K. Zhang, and L. Fu, "Enhanced-coupling-based tracking control of double pendulum gantry cranes," *International Journal of Control,*

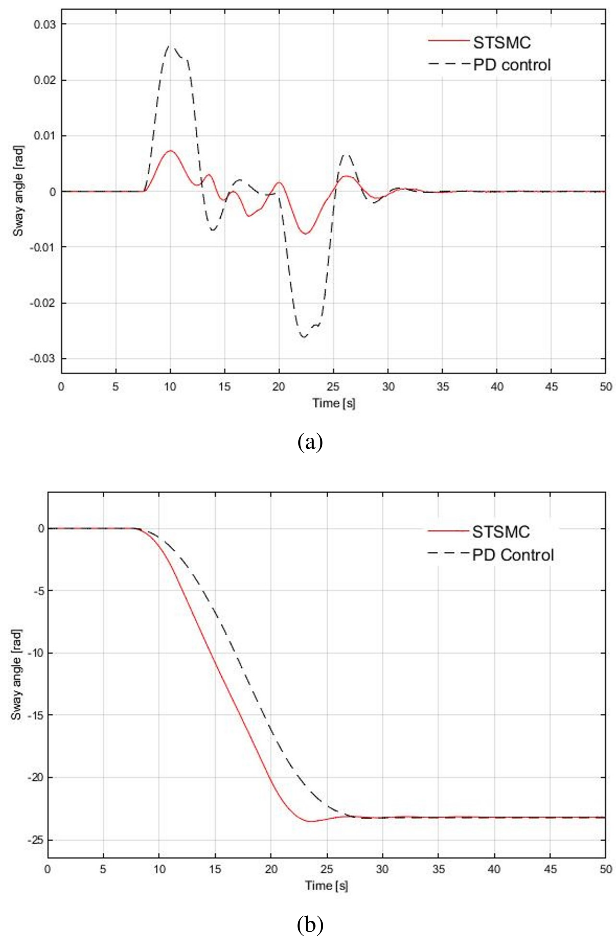

Fig. 9. Comparison of the proposed control and a PD control: (a) Sway angle and (b) traveling distance.

Automation, and Systems, vol. 20, no. 7, pp. 2260-2272, 2022.

[11] G.-H. Kim, P.-T. Pham, Q. H. Ngo, and Q. C. Nguyen, "Neural network-based robust anti-sway control of an industrial crane subjected to hoisting dynamics and uncertain hydrodynamic forces," *International Journal of Control, Automation, and Systems*, vol. 19, no. 5, pp. 1953-1961, 2021.

[12] Z. Liu, N. Sun, Y. Wu, X. Xin, and Y. Fang, "Nonlinear sliding mode tracking control of underactuated tower cranes," *International Journal of Control, Automation, and Systems*, vol. 19, no. 2, pp. 1065-1077, 2021.

[13] Q. H. Ngo, N. P. Nguyen, Q. B. Truong, and G.-H. Kim, "Application of fuzzy moving sliding surface approach for container cranes," *International Journal of Control, Automation, and Systems*, vol. 19, no. 2, pp. 1133-1138, 2021.

[14] K.-S. Hong and Q. H. Ngo, "Dynamics of the container crane on a mobile harbor," *Ocean Engineering*, vol. 53, pp. 16-24, 2012.

[15] J.-G. Sung and W. E. Singhose, "Robustness analysis of input shaping commands for two-mode flexible systems," *IET Control Theory Application*, vol. 3, no. 6, pp. 722-730, 2009.

[16] J. Vaughan, A. Y. Yano, and W. Singhose, "Robust negative input shapers for vibration suppression," *Transactions of ASME, Journal of Dynamic Systems, Measurement and control*, vol. 131, no. 3, pp. 031014.1-031014.9, 2009.

[17] P. Dadone and H. Vanlandingham, "Load transfer control for a gantry crane with arbitrary delay constraints," *Journal of Vibration and Control*, vol. 8, pp. 135-158, 2002.

[18] U. H. Shah and K.-S. Hong, "Input shaping control of a nuclear power plant's fuel transport system," *Nonlinear Dynamics*, vol. 77, no. 4, pp. 1737-1748, 2014.

[19] U. H. Shah, K.-S. Hong, and S.-H. Choi, "Open-loop vibration control of an underwater system: Application to refueling machine," *IEEE/ASME Transactions on Mechatronics*, vol. 22, no. 4, pp. 1622-1632, 2017.

[20] M. Piao, U. H. Shah, J.-Y. Jeon, and K.-S. Hong, "Input shaping control of a refueling system operating in water," *Journal of Institute of Control, Robotics and Systems*, vol. 20, no. 4, pp. 402-407, 2014.

[21] M. Piao, G.-H. Kim, U. H. Shah, and K.-S. Hong, "Dynamics analysis and residual vibration control of an overhead shuttle system," *Journal of Institute of Control, Robotics and Systems*, vol. 22, no. 6, pp. 445-452, 2016.

[22] K.-T. Hong, C.-D. Huh, and K.-S. Hong, "Command shaping control for limiting the transient sway angle of crane systems," *International Journal of Control, Automation, and Systems*, vol. 1, no. 1, pp. 43-53, 2003.

[23] Q. Ngo and K.-S. Hong, "Adaptive sliding mode control of container cranes," *IET Control Theory and Applications*, vol. 6, no. 5, pp. 662-668, 2012.

[24] L. A. Tuan, S.-G. Lee, L. C. Nho, and D. H. Kim, "Model reference adaptive sliding mode control for three dimensional overhead cranes," *International Journal of Precision Engineering and Manufacturing*, vol. 14, no. 8, pp. 1329-1338, 2013.

[25] W. He, S. S. Ge, B. V. E. How, Y. S. Choo, and K.-S. Hong, "Robust adaptive boundary control of a flexible marine riser with vessel dynamics," *Automatica*, vol. 47, no. 4, pp. 722-732, 2011.

[26] W. He, S. Zhang, and S. S. Ge, "Adaptive control of a flexible crane system with the boundary output constraint," *IEEE Transactions on Industrial Electronics*, vol. 61, no. 8, pp. 4126-4133, 2014.

[27] M. H. Nguyen, H. V. Dao, and K. K. Ahn, "Adaptive robust position control of electro-hydraulic servo systems with large uncertainties and disturbances," *Applied Sciences*, vol. 12, no. 2, pp. 1-21, 2022.

[28] T. Yang, N. Sun, and Y. Fang, "Neuroadaptive control for complicated underactuated systems with simultaneous output and velocity constraints exerted on both actuated and unactuated states," *IEEE Transactions on Neural Networks and Learning Systems*, vol. 34, no. 8, pp. 4488-4498, 2023.

[29] T. Yang, N. Sun, and Y. Fang, "Adaptive fuzzy control for a class of MIMO underactuated systems with plant uncertainties and actuator deadzones: design and experiments," *IEEE Transactions on Cybernetics*, vol. 52, no. 8, pp. 8213-8226, 2022.

[30] C. Li and C.-Y. Lee, "Fuzzy motion control of an auto-warehousing crane system," *IEEE Transactions on Industrial Informatics*, vol. 48, no. 5, pp. 983-994, 2001.

[31] Q. H. Ngo, N. P. Nguyen, and K.-S. Hong, "Fuzzy sliding mode control of container cranes," *International Journal of Control, Automation, and Systems*, vol. 13, no. 2, pp. 419-425, 2015.

[32] Q. H. Ngo, N. P. Nguyen, and K.-S. Hong, "Fuzzy sliding mode control of an offshore container crane," *Ocean Engineering*, vol. 140, pp. 125-134, 2017.

[33] S. Jarosloaw, "Fuzzy crane control with sensorless payload deflection feedback for vibration reduction," *Mechanical System and Signal Processing*, vol. 46, no. 1, pp. 70-81, 2014.

[34] X. J. Shao, J. G. Zhang, X. L. Zhang, Z. C. Zhao, and Z. M. Chen, "A novel anti-swing and position control method for overhead crane," *SAGE Journals*, vol. 103, no.1, pp. 1-24, November 2019.

[35] X. J. Shao, J. G. Zhang, and X. L. Zhang, "Takagi-sugeno fuzzy modeling and PSO-based robust LQR anti-swing control for overhead crane," *Mathematical Problems in Engineering*, vol. 2019, no. 4596782, 2019.

[36] Q. H. Ngo and K.-S. Hong, "Sliding mode anti-sway control of an offshore container crane," *IEEE-ASME Transactions on Mechatronics*, vol. 17, no. 2, pp. 201-209, 2012.

[37] Y. Wang and M. Chen, "Fixed-time disturbance observer-based sliding mode control for mismatched uncertain systems," *International Journal of Control, Automation, and Systems*, vol. 20, no. 9, pp. 2792-2804, 2022.

[38] T. N. Truong, A. T. Vo, and H.-J. Kang, "An adaptive terminal sliding mode control scheme via neural network approach for path-following control of uncertain nonlinear systems," *International Journal of Control, Automation, and Systems*, vol. 20, no. 6, pp. 2081-2096, 2022.

[39] M. H. Nguyen, H. V. Dao, and K. K. Ahn, "Extended sliding mode observer-based high accuracy motion control for uncertain electro-hydraulic systems," *International Journal of Robust and Nonlinear Control*, vol. 33, no. 2, pp. 1351-1370, 2023.

[40] D. T. Tran, D. X. Ba, and K. K. Ahn, "Adaptive backstepping sliding mode control for equilibrium position tracking of an electrohydraulic elastic manipulator," *IEEE Transactions on Industrial Electronics*, vol. 67, no. 5, pp. 3860-3869, 2020.

[41] Z. Xu, X. Yang, W. Zhang, W. Zhang, L. Zhang, and P. X. Liu, "Backstepping sliding mode control based on extended state observer for robotic manipulators with lugre friction," *International Journal of Control, Automation, and Systems*, vol. 20, no. 6, pp. 2054-2066, 2022.

[42] C. Vazquez, J. Collado, and L. Fridman, "Super twisting control of a parametrically excited overhead crane," *Journal of The Franklin Institute*, vol. 351, pp. 2283-2298, 2014.

[43] N. Sun, Y. Fang, H. Chen, and Y. Fu, "Super-twisting-based antiswing control for underactuated double pendulum cranes," *Proc. of IEEE International Conference on Advanced Intelligent Mechatronics*, pp. 749-754, 2015.

[44] J. A. Moreno and M. Osorio, "Strict Lyapunov functions for the super-twisting algorithm," *IEEE Transactions on Automatic Control*, vol. 57, no. 4, pp. 1035-1040, 2012.

[45] M. Zhai, T. Yang, N. Sun, and Y. Fang, "Under- actuated mechanical systems with both actuator and actuated/unactuated state constraints: A predictive control-based approach," *IEEE/ASME Transactions on mechatronics*, vol. 28, no. 3, pp. 1359-1371, 2023.

[46] K.-S. Hong, B.-J. Park, and M.-H Lee, "Two-stage control for container cranes," *JSME International Journal, Series C*, vol. 43, no. 2, pp. 273-282, 2000.

[47] N. B. Almutairi and M. Zribi, "Sliding mode control of a three-dimensional overhead crane," *Journal of Vibration and Control*, vol. 15, no. 11, pp. 1679-1730, 2009.

[48] K. A. Hekman and W. E. Singhose, "A feedback control system for suppressing crane oscillations with on-off motors," *International Journal of Control, Automation, and Systems*, vol. 5, no. 3, pp. 112-233, 2007.

[49] W. He and S. S. Ge, "Cooperative control of a nonuniform gantry crane with constrained tension," *Automatica*, vol. 66, pp. 146-154, 2016.

[50] H. Park, D. Chwa, and K.-S. Hong, "A feedback linearization control of container cranes: Varying rope length," *International Journal of Control, Automation, and Systems*, vol. 5, no. 4, pp. 379-387, 2007.

[51] C.-S. Kim and K.-S. Hong, "Boundary control of container cranes from the perspective of controlling an axially moving string system," *International Journal of Control, Automation, and Systems*, vol. 7, no.3, pp. 437-445, 2009.

[52] X. H. Ma and H. Q. Bao, "An anti-swing closed-loop control strategy for overhead cranes," *MDPI*, vol. 8, no.9, 2018.

[53] S. H. Zhu and N. Wang, "Hairpin RNA genetic algorithm based ANFIS for modeling overhead cranes," *Mechanical Systems and Signal Processing*, vol. 165, 2022.

[54] J. Kim, D. Lee, B. Kiss, and D. Kim, "An adaptive unscented Kalman filter with selective scaling (AUKF-SS) for overhead cranes," *IEEE Transactions on Industrial Electronics*, vol. 68, no.7, pp. 6131-6140, 2021.

[55] K.-S. Hong, L.-Q. Chen, P.-T. Pham, and X.-D. Yang, *Control of Axially Moving Systems*, Springer, ISBN 9789811629143, October 2021.

Mingxu Piao received his B.S. degree in Mechanical Engineering Department from Shanghai Maritime University, China, in 2010 and an M.S. degree in the School of Mechanical Engineering, Pusan National University, Korea, in 2019. He is currently a Ph.D. student in the School of Mechanical Engineering, Pusan National University, Korea. His research interests include system modeling, sliding mode control, adaptive control, robotics, port automation, and crane control.

Muhammad Umer Hameed Shah received his B.E. and M.S. degrees in mechanical engineering from the National University of Sciences and Technology (NUST), Pakistan, in 2005 and 2012, respectively, and a Ph.D. degree in mechanical engineering from the School of Mechanical Engineering, Pusan National University (PNU), Korea, in 2018. Currently, he is the Acting Head of Mechanical Engineering Department at the College of Engineering and Information Technology (CEIT), Ajman University (AU), United Arab Emirates (UAE). He is also a member of the Artificial Intelligence Research Center at CEIT, AU. He has held academic positions at several renowned institutions including the Lecturer position at NUST and postdoctoral positions at PNU, Texas A&M University at Qatar, and Khalifa University, UAE. His research interests include dynamics and control of underactuated systems, underwater robotics, and robotic grasping.

Guanghao Huang received his B.S. degree from the Department of Electronic Information Engineering, Jilin Institute of Chemical Technology, Jilin City, China, in 2010, an M.S. degree from the Department of Cogno-Mechatronics Engineering, Pusan National University, Busan, Korea, in 2014, and a Ph.D. degree from Department of Electronics Engineering, Pusan National University, in 2020. Since 2020, he has been an Assistant Professor with the Institute for Future, School of Automation, Qingdao University, Qingdao, China. His current research interests include systems theory, functional near infrared spectroscopy, integrated optical sensors, photonic-integrated circuits, polymeric waveguide devices, and bio-photonic sensors.

Keum-Shik Hong received his B.S. degree in mechanical design and production engineering from Seoul National University in 1979, an M.S. degree in mechanical engineering from Columbia University, New York, in 1987, and both an M.S. degree in applied mathematics and a Ph.D. degree in mechanical engineering from the University of Illinois at Urbana-Champaign in 1991. He was with the School of Mechanical Engineering, Pusan National University during 1993-2022, and is a Professor Emeritus since 2022. His Integrated Dynamics and Control Engineering Laboratory was a National Research Laboratory designated by the Ministry of Science and Technology of Korea in 2003. In 2009, under the auspices of the World Class University Program of the Ministry of Education, Science, and Technology of Korea, he established the Department of Cogno-Mechatronics Engineering, PNU. He holds a Distinguished Professorship from the Institute For Future, School of Automation, Qingdao University, Qingdao, China. He is an IEEE Fellow, a Fellow of the Korean Academy of Science and Technology, an ICROS Fellow, a Member of the National Academy of Engineering of Korea, and many other societies. Dr. Hong served as Associate Editor of Automatica (2000-2006) and an Editor-in-Chief of the Journal of Mechanical Science and Technology (JMST, 2008-2011) and the International Journal of Control, Automation, and Systems (IJCAS, 2018-2022). He was a past President of the Institute of Control, Robotics and Systems (ICROS), Korea, and the Asian Control Association (2020-2021). He was the Organizing Chair of the ICROS-SICE International Joint Conference 2009, Fukuoka, Japan. Dr. Hong received the Presidential Award of Korea (2007) and the Service Merit Medal of Korea (2022) from the Korean government. His academic awards include the Best Paper Award from the KFSTS of Korea (1999), the F. Harashima Mechatronics Award (2003), the IJCAS Scientific Activity Award (2004), the ICROS Achievement Award (2009), the IJCAS Contribution Award (2010, 2011, 2020), the Premier Professor Award (2011), the JMST Contribution Award (2011), the IEEE Academic Award (2016), etc. His current research interests include brain-computer interface, nonlinear systems theory, adaptive control, distributed parameter systems, autonomous vehicles, and innovative control applications in brain engineering.

Publisher's Note Springer Nature remains neutral with regard to jurisdictional claims in published maps and institutional affiliations.